Effect of Membrane Pore Size on the pH-Sensitivity of Polyethersulfone Hollow Fiber Ultrafiltration Membrane

Lulu Li,[1] Tao Xiang,[1] Baihai Su,[1,2] Huijuan Li,[1] Bosi Qian,[1] Changsheng Zhao[1,2,3]

[1]*College of Polymer Science and Engineering, State Key Laboratory of Polymer Materials Engineering, Sichuan University, Chengdu 610065, China*
[2]*Department of Nephrology, West China Hospital, Sichuan University, Chengdu 610041, China*
[3]*National Engineering Research Center for Biomaterials, Sichuan University, Chengdu 610064, China*

Received 17 December 2010; accepted 3 March 2011
DOI 10.1002/app.34902
Published online 24 August 2011 in Wiley Online Library (wileyonlinelibrary.com).

ABSTRACT: In our recent study, pH-sensitive polyethersulfone (PES) hollow fiber membranes were prepared by blending poly (acrylonitrile-*co*-acrylic acid) (PANAA), and the electroviscous effect had great effect on the water flux change. While the question remains: is the water flux change caused by the electroviscous effect for all the membranes with different pore sizes? Herein, pH-sensitive hollow fiber membranes with different pore sizes were prepared. The pore size and the theoretic water flux were calculated through the ultrafiltration of polyethylene glycol (PEG) solution. Comparing the calculated fluxes and the experimental ones, we found that the water flux change was mainly caused by the pore size change at the pH value larger than pKa, while that was caused by both the pore size change and the electroviscous effect when pH value was smaller than the pKa, and the pore size change was caused by the ionization of the —COOH in the copolymer. © 2011 Wiley Periodicals, Inc. J Appl Polym Sci 123: 2320–2329, 2012

Key words: polyethersulfone; hollow fiber membranes; pH-sensitive; poly (acrylonitrile-*co*-acrylic acid); electroviscous effect; pore size

INTRODUCTION

Polymeric materials are widely used as stimuli-responsive membranes in drug delivery,[1–7] and separation process,[8–14] including salt separation, water purification, and separation of ethanol-water solution, and so on. The process occurred via the abrupt property changes in response to small changes in external stimuli such as temperature, pH, ion and/or solvent composition of the media, concentration of special chemical species, electric field, and photo-irradiation.[15] Compared with other external stimuli, pH-sensitivity gives more choices both for the materials and applying environment as a novel and powerful technique.

In our recent studies,[16–20] pH-sensitive polyethersulfone (PES) hollow fiber membranes were prepared by blending copolymers containing acrylic acid (AA) chains via dry-wet spinning technique. The membranes showed evident pH sensitivity, and the electroviscous effect had great effect on the water flux. Our question was whether the water flux change was caused by the electroviscous effect for all the membranes with different pore sizes.

As we know, the PES and PES-based membranes can be used for microfiltration, ultrafiltration, nanofiltration and reverse osmosis, and the membrane pore size could be controlled by additives to the casting solution and by changes in the membrane formation process as well as by the combinations thereof.[21–23] These inspired us to focus on the study of the effect of the membrane pore size on the pH sensitivity, and the relationship between the membrane pore size and the electroviscous effect for PES hollow fiber membranes.

In recent years, many studies have been published related to the electroviscous effect. Nilsson et al.[24] evaluated the influence of pH, salt and temperature on the performance of a nanofiltration membrane to elucidate the mechanisms influencing the membrane performance at ambient and elevated temperatures, and they found that the electroviscous effect existed and was weak at low pH comparing with higher pH. Adachi[25] and Rattanakawin[26] studied the electroviscous effect for suspensions, and the results indicated that there were three distinctive regimes of the electroviscous effect for the solutions. Jiang et al.[27] found that the electroviscous effect of dilute sodium poly (styrene sulfonate) solution was subjected to a simple shear flow. Su et al.[28] discovered

Correspondence to: C. Zhao (zhaochsh70@scu.edu.cn or zhaochsh70@163.com).

Contract grant sponsor: National Natural Science Foundation of China; contract grant numbers: 51073105, 50973070, 30900691.

Contract grant sponsor: Sichuan Youth Science and Technology Foundation; contract grant number: 08ZQ026-038.

that high-CEC (cation exchange capacity) semectic of reduced charge smectites (RCS) resulted in suspension with higher viscosity due to the presence of larger number of particles and secondary electroviscous effect. Niels et al.[29] believed that the dominant contribution to the viscosity was dependent on the Bjerrum length stem from the electrostatic attractions, which was essentially a manifestation of the primary electroviscous effect. Saluja et al.[30] investigated the utilization of high-frequency rheology analysis for assessing protein–protein interactions in high protein concentration solution, and they believed that the electroviscous effect played a major role in governing protein behavior under the conditions of high surface charge and low ion strength.

In this study, pH-sensitive hollow fiber membranes with different pore sizes were prepared by blending the same amount of copolymer PANAA with different PES concentration solutions. The pH-sensitivity and pH-reversibility of the membranes were investigated. Through the ultrafiltration of polyethylene glycol (PEG) solution, the membrane pore sizes were calculated, and then the effect of the membrane pore size on the pH-sensitivity was investigated.

EXPERIMENTAL SECTION

Materials and reagents

Acrylic acid (AA), acrylonitrile (AN), *N*-methyl-2-pyrrollidone (NMP), polyethylene glycol (PEG-4000, PEG-10000), $BaCl_2$, and I_2 were obtained from Kelong Chemical Reagent, Chengdu, China. Polyethersulfone (PES, Ultrason E6020P, BASF Aktiengesellschaft) was the polymeric matrix to prepare hollow fiber membrane. AN and AA were pretreated by activated carbons for 2 h in order to remove the polymerization inhibitor before use, and all the other chemicals were used without further purification. Double distilled water was used throughout the studies.

Synthesis of poly (acrylonitrile-*co*-acrylic acid)

Monomers AN and AA (mass ratio of 2 : 3) were dissolved in *N*-methyl pyrrolidone (NMP) with the total monomer concentration of 30 wt %. AIBN, as the initiator, was introduced into the mixed solution at 1 wt % of the total monomer weight, and then the solution was stirred continuously until all the monomers were completely dissolved. After passing nitrogen for 15 min, polymerization was carried out in airtight container at 60°C for 24 h. The reaction was terminated by ethanol, and then washed several times with ethanol and hot deionized water respectively to remove the residual monomers and initiators thoroughly, which were confirmed by pH test and UV spectrum scanning until specific peaks were observed. The obtained copolymer was dried completely at 60°C in a vacuum oven for 72 h. The functional groups were analyzed by Fourier transform infrared spectrometer (FTIR). The intrinsic viscosity of the copolymer in *N*,*N*-dimethylformamide (DMF) was determined by Ubbelodhe-type viscometer at 30°C, and the molecular weight calculated by the Mark–Houwink equation was 52,000. The degree of the acrylic acid determined by ^{1}H-NMR spectroscopy [400 MHz, DMSO-d_6, δ (ppm)] was about 43.5%. The copolymer was prepared and characterized in detail as described previously.[16,31]

Preparation of pH-sensitive polyethersulfone hollow fiber membranes and filters

PES and the synthesized PANAA were dissolved in NMP in a glass reactor equipped with a mechanical stirrer to give clear homogeneous blended solutions, and the concentrations of the PES were 16, 18, 20, and 22 wt %, respectively, while the concentration of PANAA was remained as 0.5 wt %. Afterward, the polymer solutions were degassed and then used for the fabrication of pH-sensitive PES hollow fiber membranes by dry-wet spinning technique. All the hollow fiber membranes were stored in water bath for 24 h to remove the residual NMP and then were post-treated by 50 wt % glycerol aqueous solution for 24 h to prevent the collapse of the porous structures when they were dried. Additionally, the four kinds of hollow fiber membranes were named M-16, M-18, M-20, and M-22. The hollow fiber membrane filters were prepared by employing epoxy resin as the potting material, with an effective area of about 150 cm^2.

Determination of ion exchange capacity (IEC)

The titration technique was used to determine the IECs of the membranes. First, the hollow fiber membranes were alternately equilibrated by 0.1*M* HCl and 0.1*M* NaOH solutions for a couple of times, and washed by double distilled water in between. Then, the membranes were immersed in a 0.1*M* NaCl solution for 24 h to exchange the H^+ ions with Na^+ ions. Afterwards, the HCl solution was collected and titrated with a standard NaOH solution (0.01*M*) by using the pH meter as the indicator. The IEC is expressed in units of milliequivalents of proton atoms per gram of the dried membrane and was calculated by[32]:

$$IEC(mequiv./g) = \frac{V_{HCl}N_{HCl} - V_{NaOH}N_{NaOH}}{m_c} \times 1000 \quad (1)$$

where V_{HCl} and V_{NaOH} are the volumes of the HCl and NaOH solutions, respectively; N_{HCl} and N_{NaOH}

are the normalities of the HCl and NaOH solutions, respectively; and m_c is the weight of the dried hollow fiber membrane.

Scanning electron microscope

A JSM-5900LV (Japan) scanning electron microscope (SEM) was used to observe the asymmetric structure and the dimension of the hollow fiber membranes. To view the cross sections of the membranes, the samples were quenched by liquid nitrogen, cut with a single-edged razor blade, attached to the sample supports and coated with a gold layer.

pH sensitivity and pH reversibility

The flux response of the hollow fiber membranes to pH change was investigated by using an apparatus as described in earlier studies.[16,33] In the experiments, the pH value of the feed solution was adjusted by adding HCl or NaOH solution.

To study the pH sensitivity, aqueous solution was introduced into the filter by a blood pump with a controlled flow rate. At first, pure water was pumped to the filter with the inlet pressure of 135 mmHg and outlet pressure of 100 mmHg for 1 h to remove the residual glycerol and to get to steady state. Then, the pH dependence of the flux at the same pressure was determined at pH ranging from 2.0 to 12.0, then back from 12.0 to 2.0, and this experiment was repeated three times.

For the pH-reversibility experiment, the filter was alternatively introduced by pH 2.5 HCl and pH 11.5 NaOH solutions at the inlet pressure of 135 mmHg and outlet pressure of 100 mmHg and with short double distilled water rinsing between. The permeated solution was collected over 10 min after 10 min equilibration by the feed flow.

The flux was expressed as the hydrodynamic permeability, and can be calculated by eq. (2):

$$Flux(mL/(m^2.mmHg.h)) = \frac{V}{S.T.P} \tag{2}$$

where V is the volume of the permeated solution; S is the effective membrane area; t is the time of the solution collecting; and P is the pressure applied to the hollow fiber membrane ($P = (135 + 100)/2 = 117.5$ mmHg, which is the transmembrane pressure).

Ultrafiltration of PEG solution

To determine the pore sizes for the blended hollow fiber membranes prepared by different PES concentrations, the permeability of polyethylene glycol (PEG-4000, PEG-10000) solutions were investigated, since there was almost no PEG was adsorbed onto the PES membranes, which was confirmed by a simple PEG adsorption experiment. The feed solutions were prepared by dissolving the PEG in double distilled water with a concentration of 0.05 g/L. The PEG solution was applied to the filter by a blood pump with the inlet pressure of 135 mmHg and outlet pressure of 100 mmHg at different pH values and then the permeated solution was collected. The flux was also calculated using eq. (2) and the PEG concentration was determined by a UV-VIS spectrophotometer as described in our earlier studies,[20,34] and then the membrane pore sizes were calculated based on the theory in the next section.

THEORY

Calculation of membrane pore size

The pore size of the membrane was determined based on the hydrodynamic model.[35–39] According to the classical hydrodynamic model, the so called "pore model," the pore size of the hollow fiber membrane could be calculated using the following equation:

$$S_a = C_f/C_m = 2(1-q)^2 - (1-q)^4 \tag{3}$$

where S_a is the actual coefficient; C_f is the filtrate solute concentration; C_m is the solute concentration at the membrane; q is the radius ratio of the solute (r_s) to the membrane pore (r_p), $q = r_s/r_p$. The radius (r_s) of the solute in solution could be calculated by the equation,[40] $r_s = (3M/4\pi\rho N)^{1/3}$, where M is the molecular weight, ρ is the density and N is the Avogadro's number. The calculated radius for PEG-4000 and PEG-10000 were 11.7 and 15.8 Å, respectively.

The actual sieving coefficients (S_a) could be evaluated from the experimental data for the observed sieving coefficients ($S_o = C_p/C_b$, where C_p is the permeate concentration and C_b is the bulk concentration) using a stagnant film model[41,42]:

$$S_a = \frac{S_o}{(1-S_o)\exp(Jv/k) + S_o} \tag{4}$$

where k is the mass transfer coefficients and J_v is the volumetric filtrate flux (volume flow rate per membrane area).

Because of the concentration polarization, the actual sieving coefficient was smaller than the observed sieving coefficient, while the actual rejection coefficient was larger than the observed rejection coefficient. According to our recent study,[32] at high shear rate for a small molecular weight solute PEG,[43,44] the concentration polarization was not obvious at the experimental conditions, since the

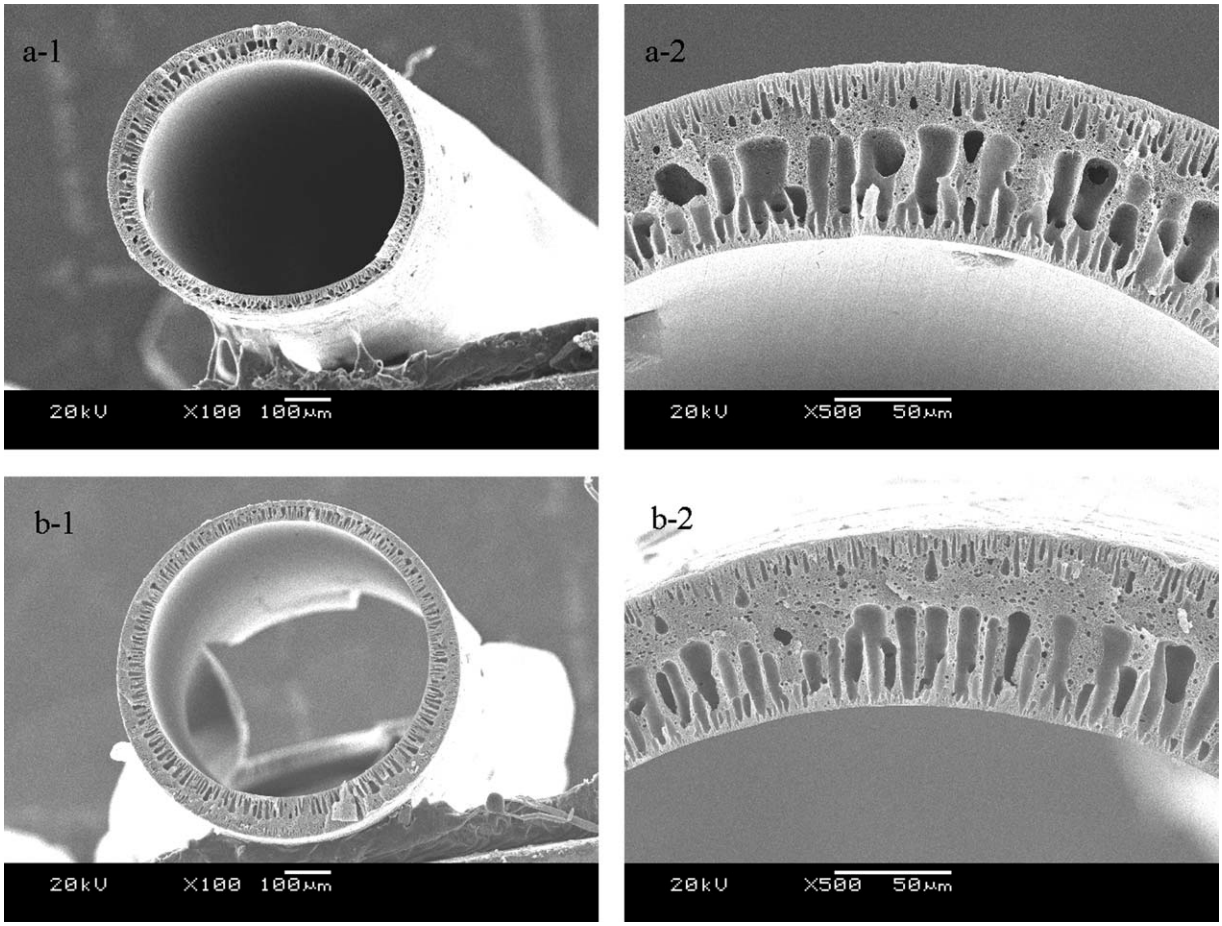

Figure 1 SEM images of the cross-section views of the membranes. Modified membranes: M-16 (a; PES 16%, copolymer 0.5%), M-18 (b; PES 18%, copolymer 0.5%), M-20 (C; PES 20%, copolymer 0.5%) and M-22 (d; PES 22%, copolymer 0.5%). Magnification: (a-d-1) 100×; (a-d-2) 500×.

adsorption of PEG on the membrane surface could be neglected. There was no obvious difference between the actual rejection coefficient and the observed rejection coefficient. Thus, the observed sieving coefficients (S_o) could be used directly to calculate the pore size using eq. (3), and the pore sizes of the membranes at different pH values were calculated.

Calculation of theoretic water permeability from pore size

The water fluxes of the membranes at different pH values could be calculated using the pore sizes calculated from eq. (3). The relationship of the water permeability and the membrane pore size could be expressed using the following equation[45]:

$$r_p = (8\mu A_x L_p / A_k)^{1/2} \quad (5)$$

where μ is the viscosity of water; A_x is the membrane thickness; A_k is the membrane surface porosity; and L_p is the hydraulic permeability (water flux). Thus, the L_p could be calculated using the transformation of the equation above as following.

$$L_p = r_p^2 A_k / 8\mu A_x \quad (6)$$

Assume that the membrane surface porosity (A_k), the viscosity of water (μ) and the membrane thickness (A_x) are constants, and do not change with the pH variation, the water fluxes of the same membrane at different pH values could be calculated based on the water flux and the membrane pore size at the pH 7. It should be noticed that the calculated water fluxes were not the fluxes at the corresponding pH values, but the fluxes at the corresponding pore radius when the membranes had no charge.

RESULTS AND DISCUSSION

SEM of the hollow fiber membrane

The microstructure and morphology of the hollow fiber membrane were investigated using scanning electron microscopy (SEM). Figure 1 shows the SEM

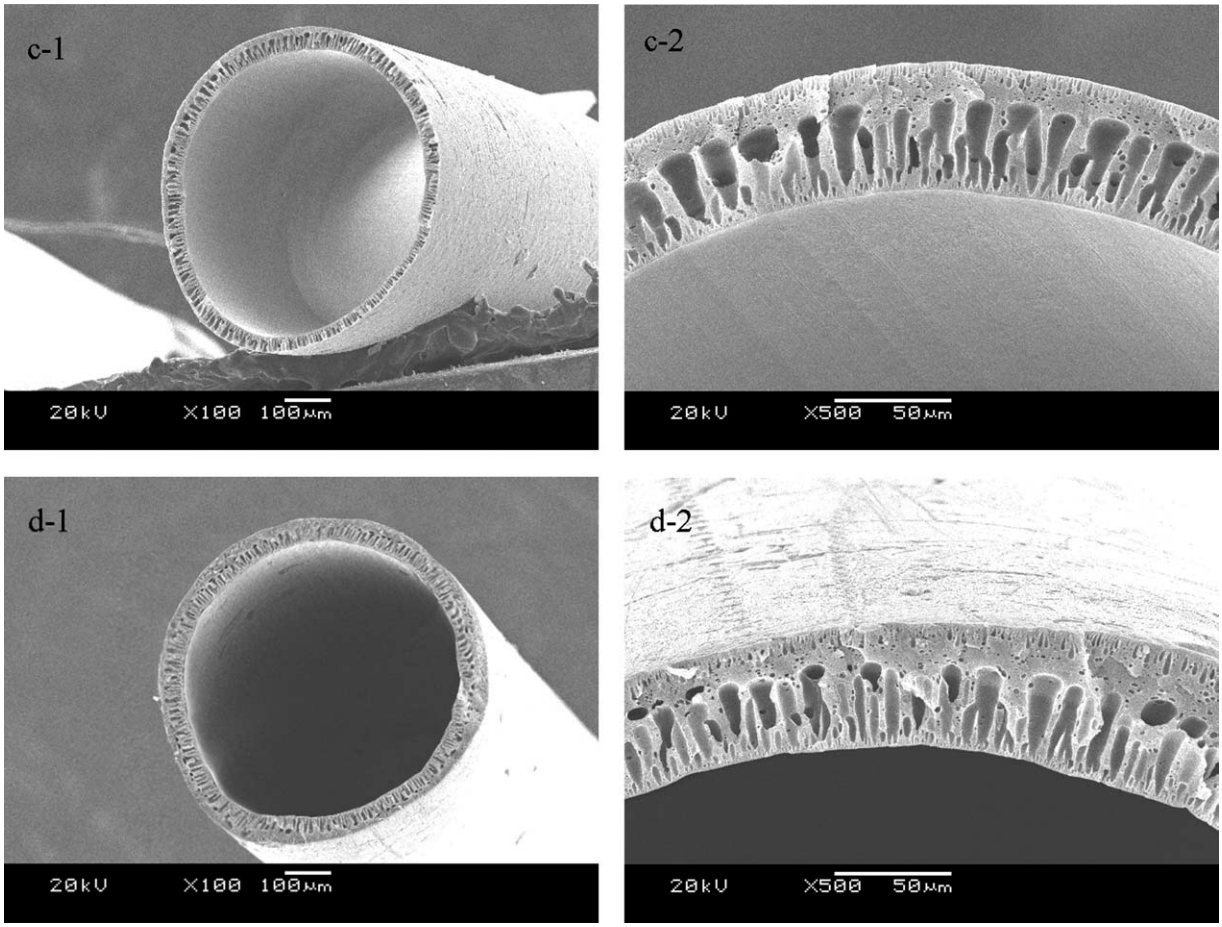

Figure 1 (Continued)

micrographs of the cross-section views of the hollow fiber membranes. The wall thickness of the hollow fiber was about 70 μm, and the inner-diameter was about 600 μm. A skin layer was found on both sides of the membrane wall, under which followed was a finger-like structure and then the porous structure. This was caused by the exchange between the solvent NMP and water during the membrane formation. The exchange occurred rapidly from the internal side of the nascent hollow fiber membrane when the polymer solution was extruded through the spinneret. After the fiber immersed in the coagulation bath, the exchange began from the outside of the membrane. Thus, a porous structure formed in the middle of the hollow fiber membrane.[46] When the PES concentration increased, the pore size decreased and the porous structure became less apparent as shown in Figure 1, and these were also proved by the calculated mean pore sizes at pH = 7, as shown in Table 1. Furthermore, the PANAA copolymer was well incorporated in the hollow fiber membrane.

TABLE I
The Mean Pore Sizes, Calculated and Titrated IECs of the Membranes

Sample	M-16	M-18	M-20	M-22
Mean pore size (10^{-10} m)[a]	39.2	33.8	27.8	13.3
Calculated IEC	0.282	0.252	0.227	0.207
Titrated IEC	0.254	0.227	0.207	0.186

[a] The mean pore size was determined at pH = 7.0 by PEG ultrafiltration.

Ion-exchange capacity

The charge property of the blended membrane was investigated in terms of membrane ion-exchange capacity (IEC). All the membranes in our study were investigated, and the pure PES membrane was considered. The calculated IECs and the titrated IECs of the four fibers are shown in Table I. The titrated IECs were about 89–91% compared with the calculated IECs. The titrated IECs are little smaller than the calculated IECs. The reason might be that when the membranes were equilibrated in the NaOH solution, the ionized carboxyl groups diminished the tendency of their neighbors to ionize. Thus, the degree of dissociation was less than 100%, resulting

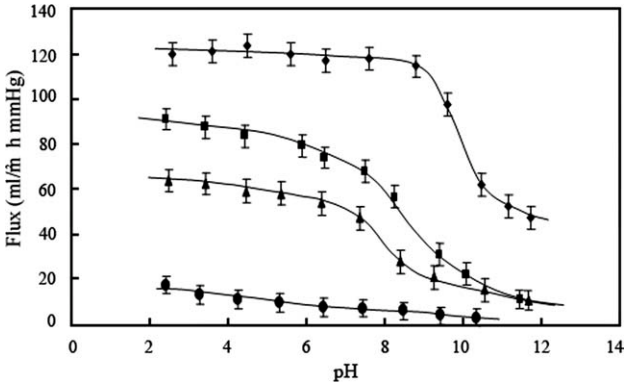

Figure 2 Water flux as a function of pH for the membranes at room temperature. Membranes: M-16 (□), M-18 (■), M-20 (▲) and M-22 (●). $n = 3$.

in the IEC difference. According to the research,[33] as more polyelectrolyte was incorporated, the space between the carboxyl groups became smaller, which resulted in a lower degree of dissociation and the increase in the IEC difference.

Membrane water flux as a function of pH value

It would be more convincing to use volume swelling ratio to quantify the swelling of pH-sensitive hydrogels, as mentioned in our earlier study for konjac glucomannan-poly(acrylic acid) IPN hydrogels.[47] In this study, the matrix of the blended membranes was polyethersulfone (PES), which can not swell or shrink, although the poly(acrylic acid) was blended into PES membrane, the amount was less than 0.5 wt %, and the volume swelling ratio was very low. Thus, the flux change was used to express the pH-sensitivity. The fluxes for the membranes (M-16, M-18, M-20, and M-22) are shown in Figure 2. As shown in the figure, the fluxes ranged from 2.3 mL/(m^2 h mmHg) to 123.6 mL/(m^2 h mmHg). With the decrease of the PES concentration, the ratio of the PANAA to PES increased, thus the fluxes increased due to the increased mean pore size (as shown in Table I) and the increased hydrophilicity as mentioned in the following section.

When the pH values changed from 2.0 to 12.0, the fluxes of the blended membranes decreased. That is to say, the fluxes showed pH dependence after blending the copolymer. When the pH values increased from 2.0 to 12.0, the flux for the M-16 decreased from 123.6 mL/(m^2 h mmHg) to 48.5 mL/(m^2 h mmHg); while that decreased from 92 mL/(m^2 h mmHg) to 10.7 mL/(m^2 h mmHg) for the M-18; and for the M-20 and M-22, the fluxes decreased from 65 mL/(m^2 h mmHg) to 10 mL/(m^2 h mmHg), and from 18 mL/(m^2 h mmHg) to 3.4 mL/(m^2 h mmHg), respectively.

The fluxes for the blended membranes exhibited obvious valve behavior at pH between 6 and 11, and hardly changed at the pH values lower than 6 for M-16 and M-22. Additionally, for M-18, a larger flux variation was observed, which varied from 92 mL/(m^2 h mmHg) at pH 2.3 to 10.7 mL/(m^2 h mmHg) at pH 11.4. According to the article,[48] the chain configuration of weak polyacid is a function of pKa of the polymer, the pKa of PAA in solution is about 4.3–4.9 dependent on the measurement method, which is not in agreement with that from Figure 2. The reason might be that the synthesized PANAA was a random copolymer, thus, the morphology of PAA chain in the copolymer was quite different from that of homopolymer PAA. At the same time, the charge density was lower in the copolymer than that in the homopolymer PAA due to the AN chains, which affected the transformation from carboxyls to carboxylate ions; and thus resulted in the difference in the pKa values. Furthermore, there was no significant difference for the fluxes at a same pH value when the pH ranging from 2.0 to 12.0 and from 12.0 to 2.0; and the results were different from the research of Sahoo et al.[49] The reason might be that the amount of the acrylic acid was larger than that in the blended membranes in this study.

In our previous studies,[16–20] it was found that with the increase of the copolymer amounts, the flux increased. In this study, the amounts of the copolymer were the same but the concentrations of PES were different, which led to the different ratios of PANAA to PES. Thus, the IECs and the pore sizes were different, which affected the water flux changes.

Membrane pH reversibility

To further study the function of the membranes, the pH-reversibility of the membranes was evaluated by buffer solution fluxes at pH 2.5 and 11.5. Each flux

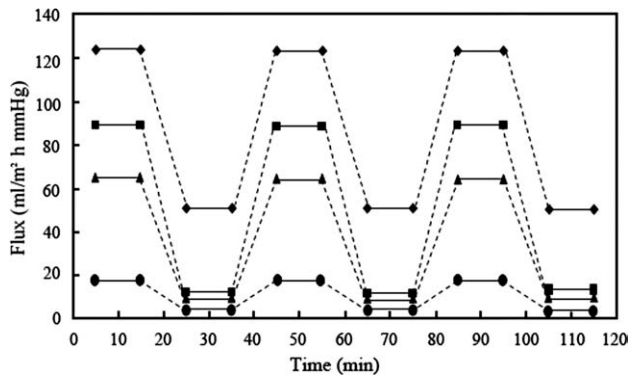

Figure 3 Hydrodynamic permeability for the blended membranes as the feed solution was exchanged between pH 2.5 and 11.5 with 10 min equilibration flow followed by 10 min sample collecting. Membranes: M-16 (◆), M-18 (■), M-20 (▲) and M-22 (●). Duplicate experiments showed similar results.

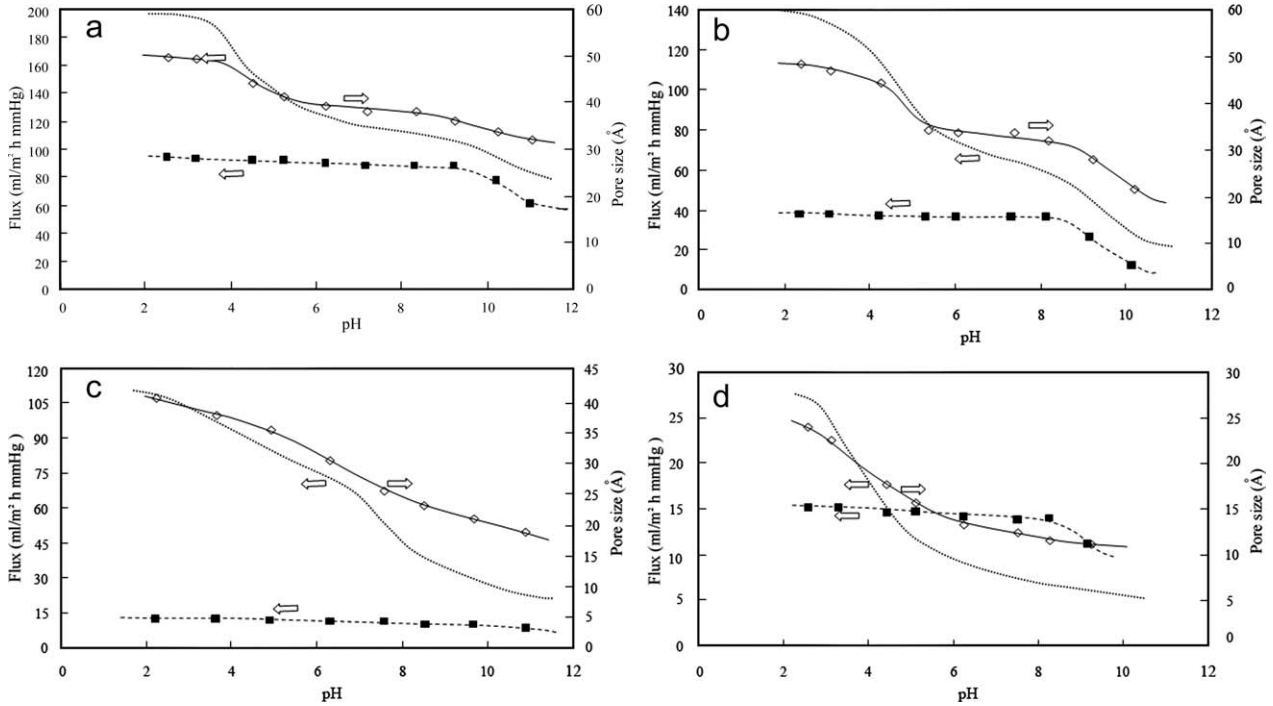

Figure 4 PEG flux change, the calculated pore size and the pure water permeability calculated from the pore size for the membranes at different pH values. The broken line is for the calculated water permeability; (□) is for the pore size; (■) is for the PEG flux change. Membranes: M-16 [Fig. 4(a)], M-18 [Fig. 4(b)], M-20 [Fig. 4(c)] and M-22 [Fig. 4(d)].

datum was obtained with 10-min equilibration followed by 10-min sample collection. Figure 3 shows the fluxes for the blended membranes. As shown in the figure, the flux was reversible as the solution was alternated, the fluxes were reversible between 125.0 and 55.0 mL/(m^2 mmHg h) for M-16, and 90.0 and 10.0 mL/(m^2 mmHg h) for M-18, and for the M-20 and M-22, the fluxes were reversible between 65 mL/(m^2 mmHg h) and 10 mL/(m^2 mmHg h), 18 mL/(m^2 mmHg h) and 3.4 mL/(m^2 mmHg h), respectively. And the multiples of the fluxes change were 2.3, 9.0, 6.5, and 5.3, respectively.

For M-16, the IEC was the highest; however, the membrane pore size was very large as shown in the SEM pictures and in Table I. When the pH values changed from 2.5 to 11.5, the pore size change ratio was the smallest, thus the water flux change was the smallest. For M-22, when the pH value changed from 2.5 to 11.5, though the pore size change ratio was very large, both the IEC and the charge density were the smallest, thus the water flux change was not the largest. These results indicated that both the pore size and the IEC had great effect on the water flux change; and these led to that when the PES concentration was at 18–20 wt% in this study, the water flux change was very large.

The PANAA copolymer was blended with PES, and incorporated in the PES membrane, i.e., the PANAA dispersed within the PES matrix. The carboxylic acids of AA could dissociate to carboxylate ions at pH 11.5 to provide high charge density in the copolymer,[36] and the copolymer would be swelling, which blocked the solution flow. However, the PAN chains restricted the movement of the copolymer, thus the swelling might be small.

The pore size and the calculated flux as a function of pH value

The water fluxes could be calculated using the pore size data by eq. (6). The PEG solution flux change, the pore size change and the calculated water flux change for the membranes at different pH values are shown in Figure 4.

As shown in Figure 4, when the pH values changed from 2.0 to 12.0, the PEG solution flux for M-16 decreased from 91.5 to 60.4 mL/(m^2 h mmHg), while that decreased from 37.9 to 11.8 ml/(m^2 h mmHg) for M-18; and for M-20 and M-22, the fluxes decreased from 11.9 to 5.0 mL/(m^2 h mmHg) and from 14.7 to 10.9 mL/(m^2 h mmHg), respectively. However, the PEG fluxes did not change when the pH values was lower than 8.0, and they decreased markedly between 8.0 and 11.0. The PEG solution fluxes still appeared pH-sensitivity; and the pH-sensitive lag from pH 4.0–7.0 to pH 8.0–11.0 compared with water solution was observed. These might be caused by the pore size change and the electroviscous effect.

The pore size change for the membranes at different pH values are also shown in Figure 4. The pore

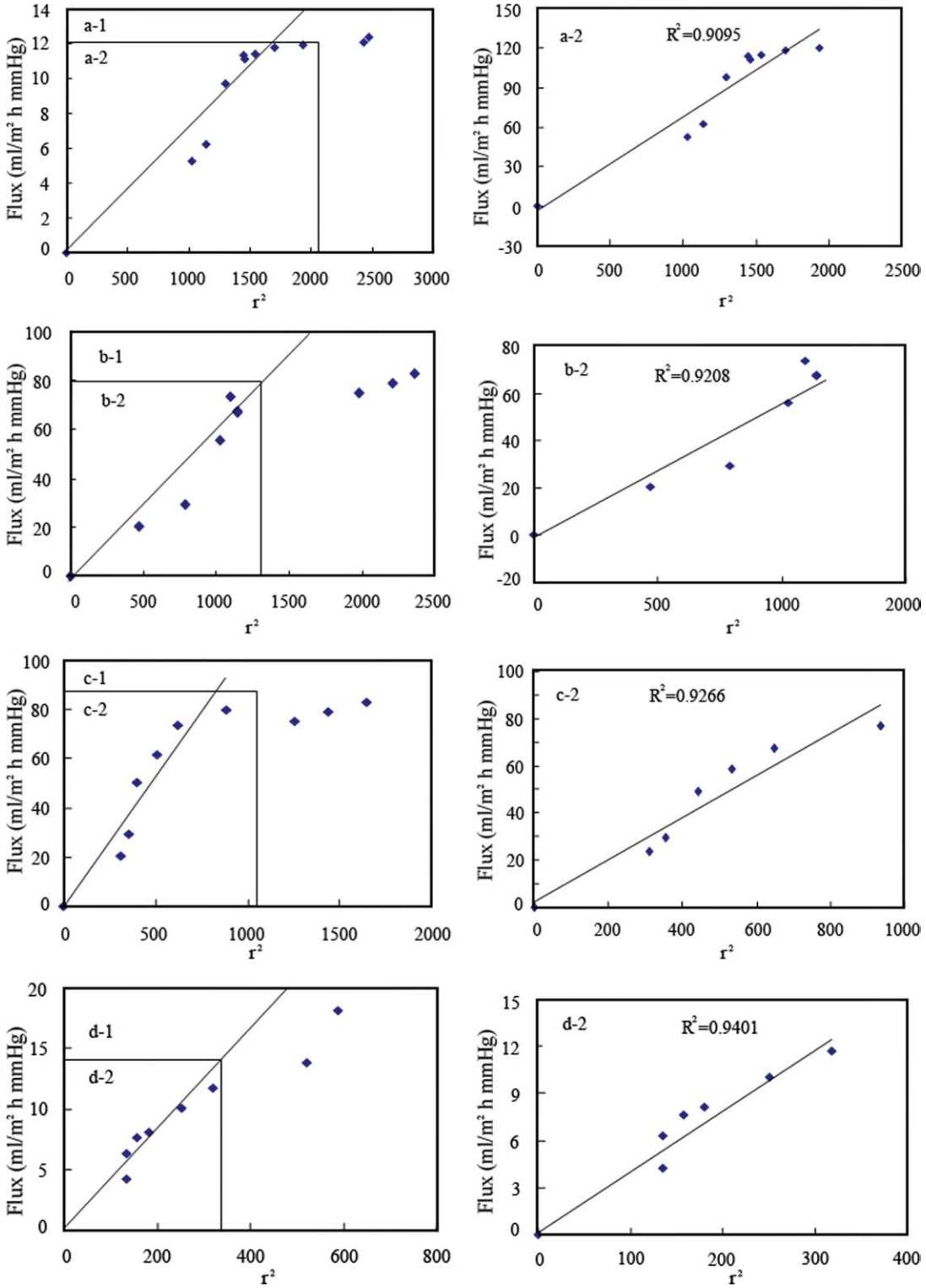

Figure 5 The relationship between the square of pore size radius and the actual water fluxes.

sizes had sharp decreases for all the membranes at the pH values between 4.0 and 7.0, and decreased gradually at the pH values exceeded 7.0, though the flux change might be not in this range. For M-16, the pore sizes changed from 50 to 33.3 Å gradually when the pH values changed from acid to basic conditions, and hardly changed at the pH values lower than 4 or higher than 7; while that decreased from 48.5 to 21.6 Å for M-18; and for M-20 and M-22, the pore sizes changed from 40.6 to 17.7 Å, and from 24.2 to 11.6 Å, respectively. It was interesting to be found that the pH value for the pore size change

was in agreement with the pKa of PAA.[48] The results suggested that the pH value of the ionization did not change even in the copolymer, and the pore size change was caused by the ionization of the —COOH in the copolymer.

Based on the pore size data, the theoretic water fluxes could be calculated as shown in Figure 4. Comparing the pure water flux in Figure 2, the calculated fluxes were different from the experimental ones. These were caused by the electroviscous effect. For the noncharged membrane, such as PES membrane, there is no change in the permeability when the solution changed from acid to basic conditions. However, for the charged membranes in this study, the membranes had charge and the charge density was very small at acid condition, but the solution had negative charges, thus the flux decreased compared with the calculated flux. At basic condition, the membrane pore had no change as indicated from the pure water permeability in the figure and mentioned above, the membranes charge density increased, thus the flux decreased. These results indicated that the electroviscous effect had great effect on the hydrodynamic permeability, which was comfortable with the electroviscous effect theory.

The pore size and experimental water flux

According to eq. (6), there was a linear relationship between the theoretic water flux and the square of the pore radius of the membrane. Figure 5 shows the relationship between the experimental flux and the square of the pore size radius. A good linear relationship was observed when the pore sizes were smaller (at basic conditions). However, when the pore sizes were larger (at acid conditions), a clear deviation from the straight line was observed. For the four blended membranes, the deviated points were at the pH value of about 4.5. It is very interesting that this pH value was the pKa of PAA in solution.[48]

The PAA could be ionized when the pH value exceeded the pKa, then the PAA stretches and becomes negatively charged. The pore surface would have lower charge density when the pH value exceeded the pKa, which was also affected by the AN chains in the copolymer. The electroviscous effect existed but the influence was smaller compared with the decreased pore diameter, and these resulted that the water flux change was mainly caused by the pore size change when the pH value exceeded the pKa, then resulted in the linear relationship. At the same time, there was rarely ionization when the pH value was lower than the pKa, the surface pore diameter changed gradually, the charge density changed a lot when an electrolyte solution was passed through a narrow capillary or pore with charged surfaces, which resulted in that the electroviscous effect took the main reason in water flux change, and the clear deviation from the straight line was observed.[50]

To explain the electroviscous effect affect more when the pore size was smaller, the flux change ratios (Lp-Flux)/Lp was used, where Lp and Flux are the theoretic water flux and experimental water flux, respectively. With the pore size decreased gradually from M-16 to M-22, the flux change ratios increased (0.330, 0.372, 0.374, and 0.417, at the pH value 3, respectively). This indicated that when the pore size was small, the "electroviscous effect" affect more.

Furthermore, when the pH value was lower than the pKa, there were no ionization and more carboxyls presented in the membranes, which resulted in the pore size increased, then appeared the significant electroviscous effect. Because of the dual effects of the pore size change and the electroviscous effect at lower pH values, it was always found that there was no significant change in water fluxes at acid conditions for most of the pH-sensitive membranes.

CONCLUTIONS

In this study, pH-sensitive polyethersulfone hollow fiber membranes with different pore sizes were prepared by blending a copolymer of acrylonitrile and acrylic acid (PANAA), and the effects of pore sizes on the pH sensitivity were investigated. When the PES concentration increased, the membrane pore size decreased, and the flux decreased. Based onthe measured pore sizes, the theoretic water fluxes for different membranes under different pH values were calculated. Comparing the calculated fluxes and the experimental ones, it could be found that the water flux change was mainly caused by the pore size change at the pH value larger than the pKa, while that was caused by both the pore size change and the electroviscous effect when the pH value was smaller than the pKa, and the pore size change was caused by the ionization of the —COOH in the copolymer.

The authors thank their laboratory members for their generous help.

References

1. Li, F.; Liu, W. G.; Yao, K. D. Biomaterials 2002, 23, 343.
2. Drummond, D. C.; Zignani, M.; Leroux, J. C. Prog Lipid Res 2000, 39, 409.
3. Park, S. B.; You, J. O.; Park, H. Y.; Haam, S. J.; Kim, W. S. Biomaterials 2001, 22, 323.
4. Kyriakides, T. R.; Cheung, C. Y.; Murthy, N.; Bornstein, P.; Stayton, P. S.; Hoffman, A. S. J Control Release 2002, 78, 295.
5. Shieh, M. J.; Lai, P. S.; Young, T. H. J Membr Sci 2002, 204, 237.

6. Mrsny, R. J. J Control Release 1992, 22, 15.
7. Watts, P. J.; Lllum, L. Drug Dev Ind Pharm 1997, 23, 893.
8. Berezina, N. P.; Kononenko, N. A.; Dyomina, O. A.; Gnusin, N. P. Adv Colloid Interface 2008, 139, 3.
9. Bandini, S.; Drei, J.; Vezzani, D. J Membr Sci 2005, 264, 65.
10. Hsueh, C. L.; Kuo, J. F.; Huang, Y. H.; Wang, C. C.; Chen, C. Y. Sep Purif Technol 2005, 41, 39.
11. Mika, A. M.; Childs, R. F.; Dickson, J. M. J Membr Sci 2002, 206, 19.
12. Zhao, C. S.; Wei, Q. R.; Yang, K. G.; Liu, X. D.; Nomizu, M.; Nishi, N. Sep Purif Technol 2004, 40, 297.
13. Zhao, C. S.; Liu, X. D.; Nomizu, M.; Nishi, N. J Colloid Interface Sci 2004, 275, 470.
14. Strathmann, H. AICHE J 2001, 47, 1077.
15. Gong, C. B.; Lam, M. H. W.; Yu, H. Y. Adv Funct Mater 2006, 16, 1759.
16. Qian, B. S.; Li, J.; Wei, Q.; Bai, P. L.; Fang, B. H.; Zhao, C. S. J Membr Sci 2009, 344, 297.
17. Zhao, C. S.; Yu, B. Y.; Qian, B. S.; Wei, Q.; Yang, K. G.; Zhang, A. M. J Membr Sci 2008, 310, 38.
18. Wei, Q.; Li, J.; Qian, B. S.; Fang, B. H.; Zhao, C. S. J Membr Sci 2009, 337, 266.
19. Li, L. L.; Yin, Z. H.; Li, F. L.; Xiang, T.; Chen, Y.; Zhao, C. S. J Membr Sci 2010, 349, 56.
20. Xiang, T.; Zhou, Q. H.; Li, K.; Li, L. L.; Su, F. F.; Qian, B. S.; Zhao, C. S. Separ Sci Technol 2010, 45, 1.
21. Boom, R. M.; van den Boomgard, T.; Smolders, C. A. J Membr Sci 1994, 90, 231.
22. Rana, D.; Matsuura, T.; Narbaitz, R. M.; Feng, C. J Membr Sci 2005, 249, 103.
23. Wang, Y.; Wang, T.; Su, Y.; Peng, F.; Wu, H.; Jiang, Z. Langmuir 2005, 21, 11856.
24. Nilsson, M.; Trägårdh, G.; Östergren, K. J Membr Sci 2008, 312, 97.
25. Adachi, Y.; Nakaishi, K.; Tamaki, M. J Colloid Interface Sci 1998, 198, 100.
26. Rattanakawin, C. R. Hogg Miner Eng 2007, 20, 1033.
27. Jiang, L.; Yang, D. H.; Chen, S. B. Macromolecules 2001, 34, 3730.
28. Su, C. C.; Shen, Y. H. P. Colloids Surfaces A: Physicochem Eng Aspects 2005, 259, 173.
29. Mortensen, N.; Kristensen, A. A. Appl Phys Lett 2008, 92, 063.
30. Saluja, A.; Badkar, A. V.; Zeng, D. L.; Nema, S.; Kalonia, D. S. J Pharm Sci 2006, 95, 1967.
31. Fang, B. H.; Ling, Q. Y.; Zhao, W. F.; Ma, Y. L.; Bai, P. L.; Wei, Q.; Li, H. F.; Zhao, C. S. J Membr Sci 2009, 329, 50.
32. Mika, A. M.; Childs, R. F.; Dickson, J. M.; McCarry, B. E.; Gagnon, D. R. J Membr Sci 1995, 108, 37.
33. Hu, K.; Dickson, J. M. J Membr Sci 2007, 301, 19.
34. Zou, W.; Huang, Y.; Luo, J.; Liu, J. Zhao, C. S. J Membr Sci 2010, 358, 76.
35. Zhao, C. S.; Zhou, X. S.; Yue, Y. L. Desalination 2000, 129, 107.
36. Ravikovitch, P. I.; Haller, G. L.; Neimark, A. V. Adv Colloid Interface Sci 1998, 77, 203.
37. Ferry, J. D. Physiol J Gen 1936, 20, 95.
38. Verniory, A.; Du Bois, R.; Decoodt, P.; Gassee, J. P.; Lambert, P. P. J Gen Physiol 1973, 62, 489.
39. Haberman, W. L.; Sayre, R. M. David Taylor Modes Basin Report No.1143, Department of the Navy, US, 1958.
40. Durbin, R. P. J Gen Physiol 1960, 44, 315.
41. Zeman, L. J.; Zydney, A. L. Microfiltration and Ultrafiltration: Principles and Applications. Marcel Dekker Inc., 1996.
42. Mehta, A.; Zydney, A. L. J Membr Sci 2005, 249, 245.
43. Bian, R.; Yamamoto, K.; Watanabe, Y. Desalination 2000, 131, 225.
44. Bhattacharjee, C.; Datta, S. Sep Purif Technol 2003, 33, 115.
45. Childress, A.; Elimelech, M. Environ Sci Technol 2000, 34, 3710.
46. Wang, D. L.; Li, K.; Teo, W. K. J Membr Sci 1996, 115, 85.
47. Wen, X.; Cao, X. L.; Yin, Z. H.; Wang, T.; Zhao, C. S. Carbohydr Polym 2009, 78, 193.
48. Mark, H.; Gaylord, N.; Bikales, N. Encyclopaedia of Polymer Science and Technology, Interscience Publishers, 1976.
49. Sahoo, A.; Ramasubramani, K. R. T.; Jassal, M.; Agrawal, A. K. Eur Polym J 2007, 43, 1065.
50. Lai, P. S.; Shieh, M. J.; Pai, C. L.; Wang, C. Y.; Young, T. H. J Membr Sci 2006, 275, 89.